Supplementary Figure 1

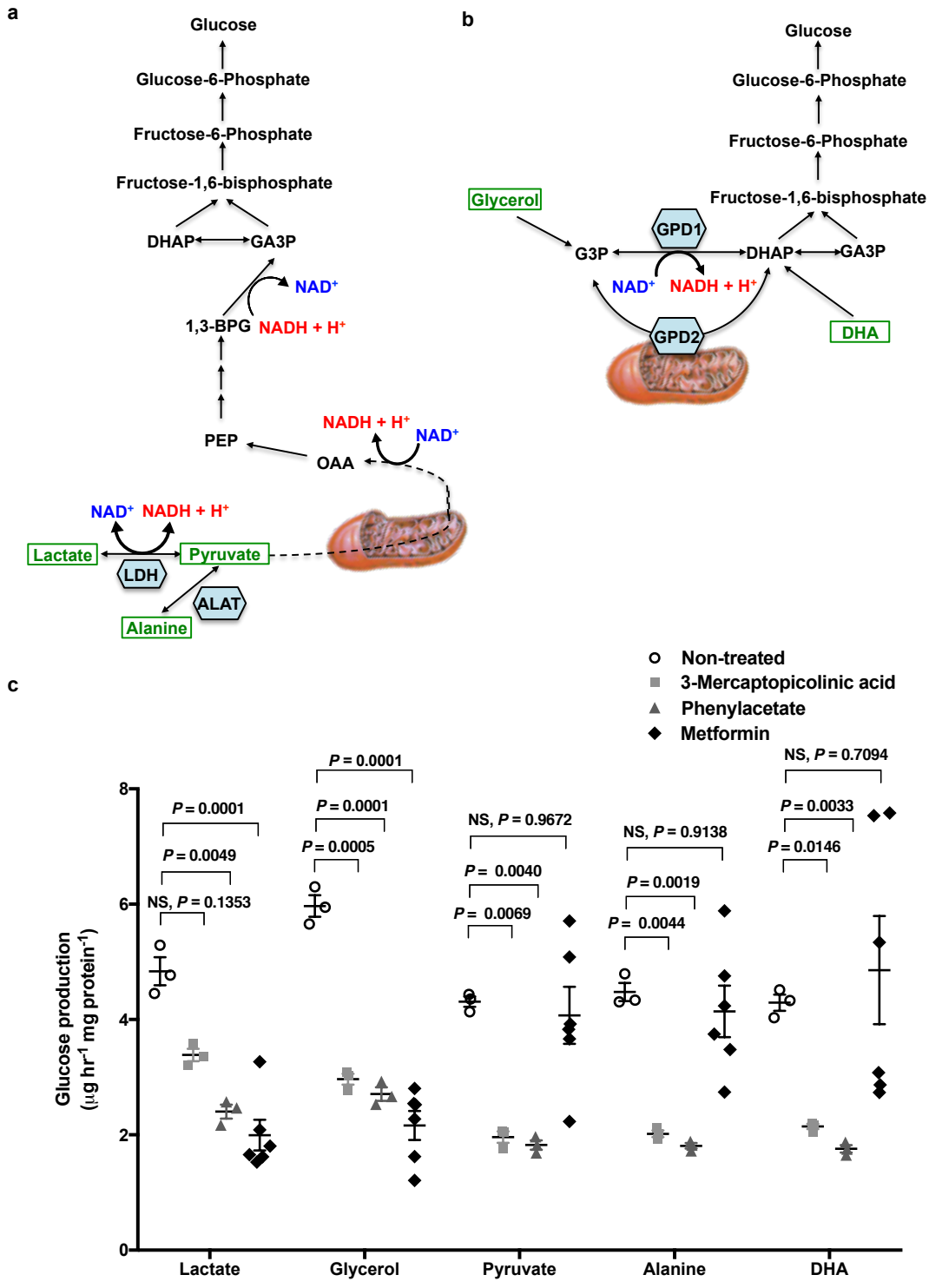

Supplementary Figure 1 Redox regulation of substrate conversion to glucose in the gluconeogenic pathway. (**a**) A schematic diagram illustrating the biochemical pathways taken by alanine and lactate when contributing to the pyruvate pool in hepatocytes. Alanine is converted to pyruvate by alanine aminotransferase (ASAT) without altering the cytosolic [NADH]:[NAD^+] ratio. Lactate is converted to pyruvate by lactate dehydrogenase (LDH) and in the process reduces the cytosol (e.g. increases the [NADH]:[NAD^+] ratio). Pyruvate itself can enter gluconeogenesis via pyruvate carboxylase (PC), which converts it to oxaloacetate (OAA), and phosphoenolpyruvate carboxykinase (PEPCK), which converts OAA to phosphoenolpyruvate (PEP). These

steps do not alter the cytosolic redox state. (**b**) A schematic diagram mapping the route of glycerol as a substrate for gluconeogenesis in hepatocytes. Glycerol must be converted to glycerol-3-phosphate (G-3-P) by glycerol kinase, and G-3-P must either be catalyzed by either mitochondrial glycerophosphate dehydrogenase (GPD2) or the cytosolic glycerophosphate dehydrogenase (GPD1) to dihydroxyacetone phosphate (DHAP). Catalysis by GPD1 will increase cytosolic redox state. Dihydroxyacetone (DHA) can be converted by dihydroxyacetone kinase (DAK) to DHAP, which will contribute to gluconeogenesis without affecting redox state. (**c**) Glucose production measured from various gluconeogenic substrates, and the impact of the chemical inhibitor of PCK-C (300 μM 3-mercaptopicolinic acid), inhibitor of PC (4 mM phenylacetate) or 100 μM metformin on substrate-mediated glucose production from isolated primary rat hepatocytes in culture. Data are mean ± SEM, (Non-treat; n = 3 per substrate; 3-mercaptopicolinic acid: n = 3 per substrate; phenylacetate: n = 3 per substrate; metformin: n = 6 per substrate; technical replicates, individual cultures in a single experiment). For statistical analysis, P values were calculated by two-way *ANOVA* with Dunnett's multiple comparisons test, and NS = Not significant (**c**).

Supplementary Figure 2

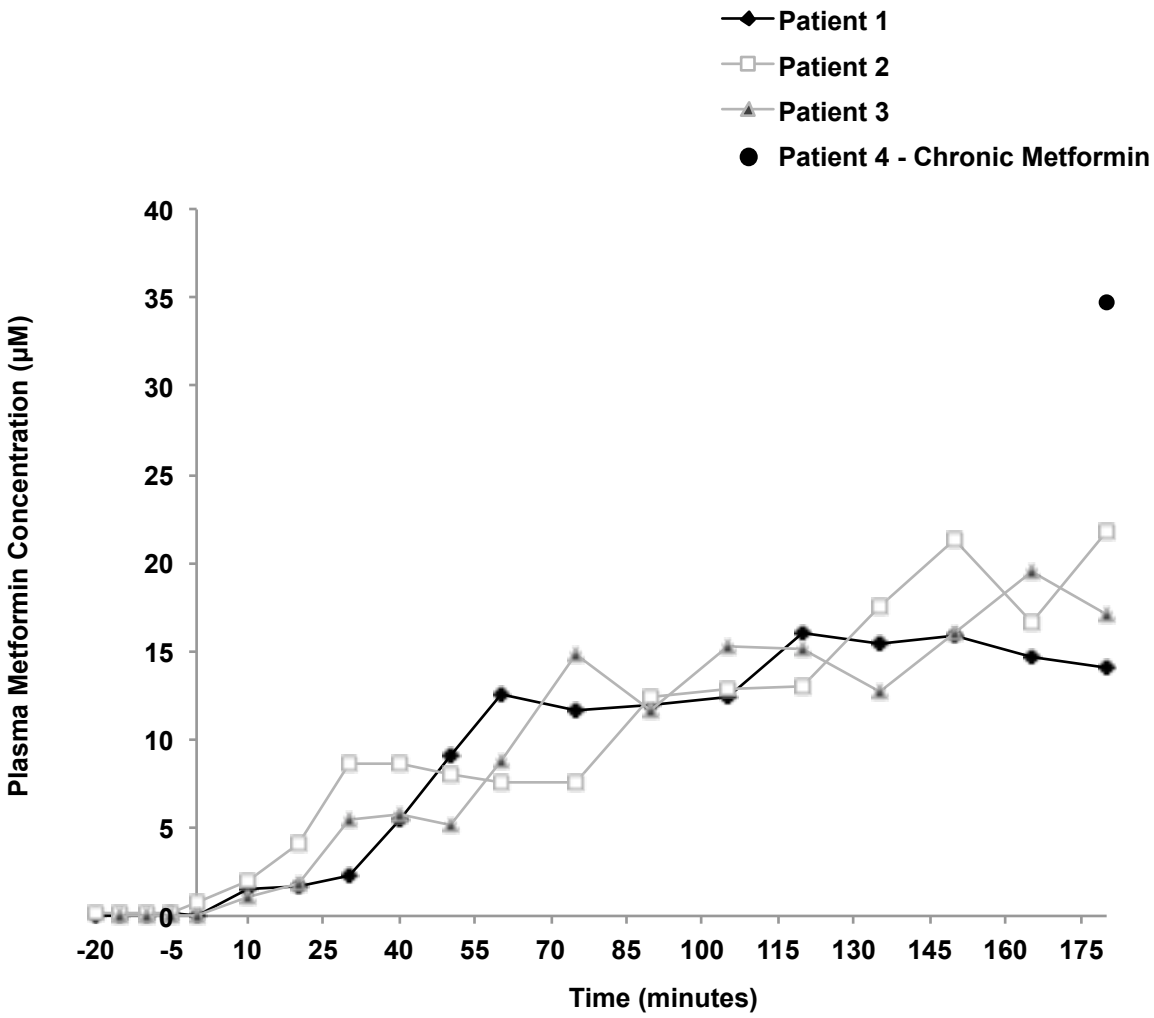

Supplementary Figure 2 Plasma metformin concentrations in individuals with type 2 diabetes following acute and chronic oral metformin administration. Individuals (n=3) with type 2 diabetes were administered 1 g metformin orally at t = 0 minutes and plasma metformin concentrations were measured over the next 3 hours every 10 minutes. The plasma sample for the chronic metformin study was obtained from an individual with type 2 diabetes who was taking chronic metformin (1g orally twice a day). Time points left of zero on the x-axis are plasma metformin measurements made prior to acute administration of the oral metformin dose.

Supplementary Figure 3

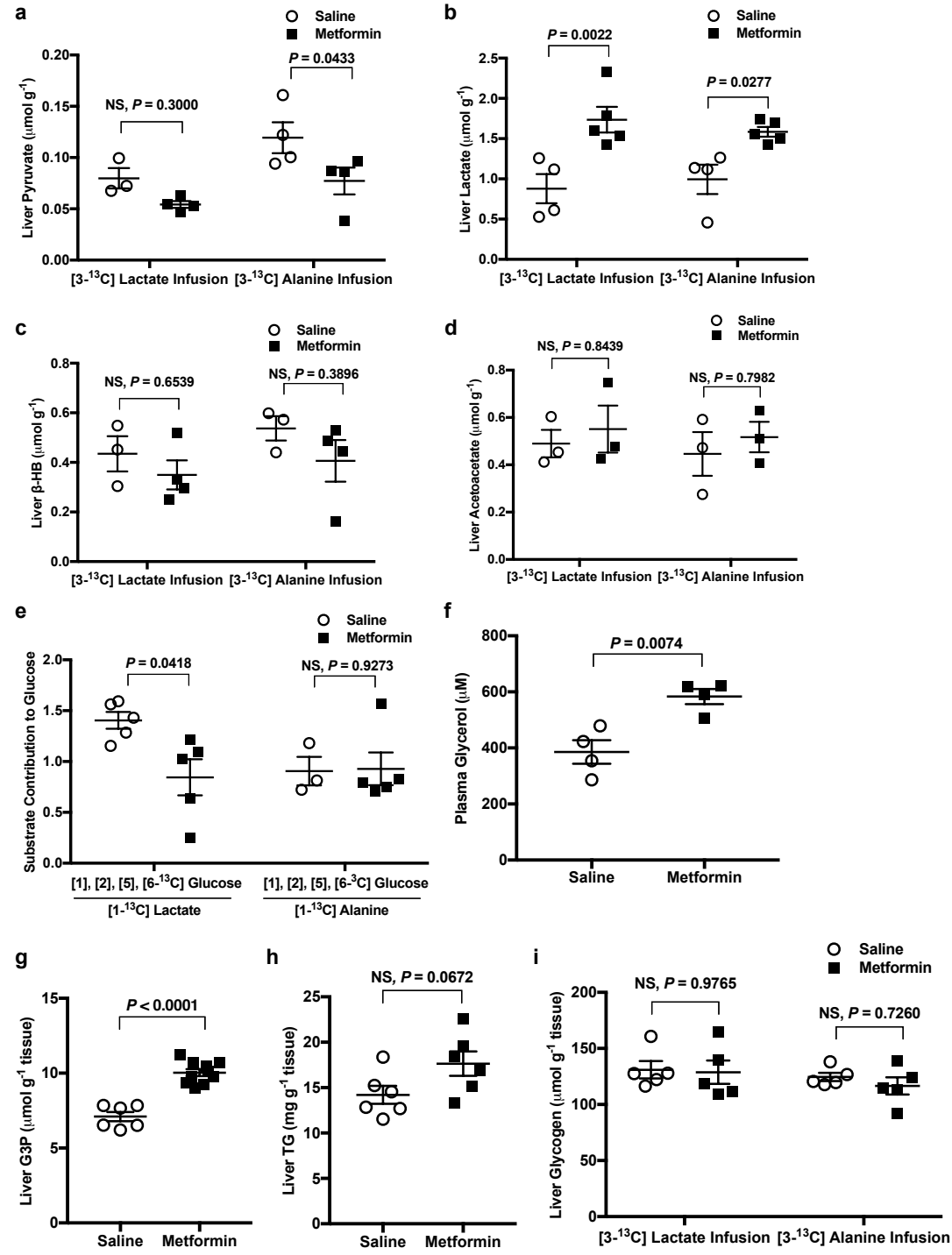

Supplementary Figure 3 Effect of acute IV 50 mg kg^{-1} metformin treatment on liver substrate concentrations in SD rats. (**a**) Liver pyruvate concentration measured from SD rats 2 h following acute IV metformin treatment or saline control in the [3-^{13}C]lactate and [3-^{13}C]alanine tracer infusion cohorts. (**b**) Liver lactate concentrations 2 h post-metformin or saline in SD rats from both tracer infusions. (**c**) Hepatic β-hydroxybutyrate concentration and (**d**) liver acetoacetate concentration in rats treated with metformin or saline from both infusion studies. (**e**) Individual substrate contribution of lactate to glucose indicated by the labeling of glucose in positions 1, 2, 5 and 6 by [3-^{13}C]lactate, and of alanine determined by labeling of glucose by [3-^{13}C]alanine in metformin or saline treated rat liver. (**f**) Plasma glycerol concentration, (g) liver G-3-P concentration, (**h**) liver triglyceride levels and (**i**) hepatic glycogen levels in metformin and saline treated rats from both tracer infusion cohorts. Data are mean ± SEM, (For (**a**): [3-^{13}C] lactate, saline n = 3, metformin n = 4, [3-^{13}C] alanine saline n = 4,

metformin n = 4; for (**b**): [3-^{13}C] lactate saline n = 4, metformin n = 5, [3-^{13}C] alanine saline n = 5, metformin n = 5; for (**c**): [3-^{13}C] lactate saline n = 3, metformin n = 4, [3-^{13}C] alanine saline n = 3, metformin n = 4; for (**d**): [3-^{13}C] lactate saline n = 3, metformin n = 3, [3-^{13}C] alanine saline n = 3, metformin n = 3; for (**e**): [3-^{13}C] lactate saline n = 5, metformin n = 5, [3-^{13}C] alanine saline n = 3, metformin n = 5; for (**f**): saline n = 4, metformin n = 4; for (**g**): saline n = 6, metformin n = 10; for (**h**): saline n = 6, metformin n = 6; for (**i**): [3-^{13}C] lactate saline n = 5, metformin n = 5, [3-^{13}C] alanine saline n = 5, metformin n = 5; biological replicates). For statistical analysis, P values were calculated by two-way *ANOVA* and NS = Not significant.

Supplementary Figure 4

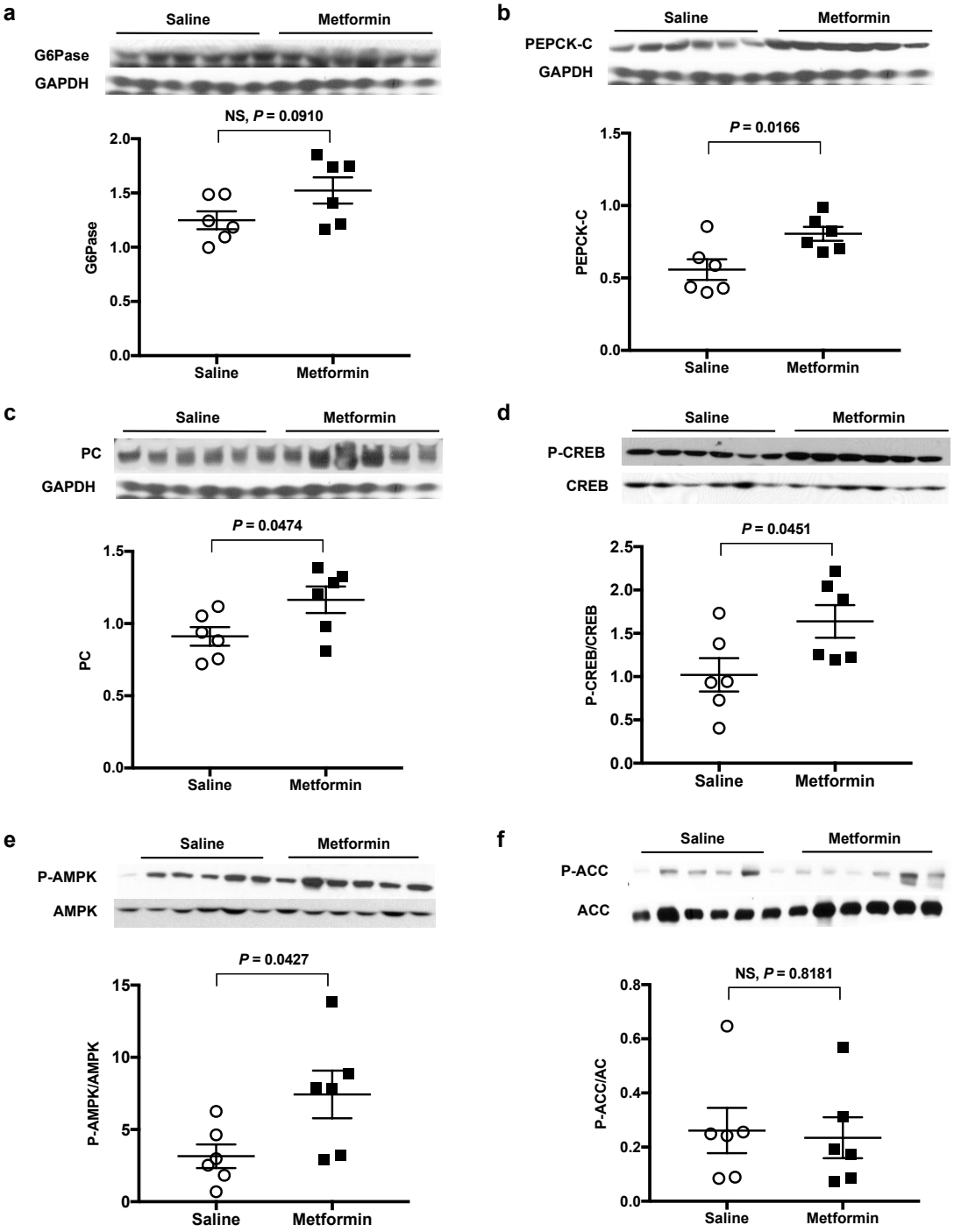

Supplementary Figure 4 Effect of acute IV 50 mg kg^{-1} metformin treatment on the protein expression of liver gluconeogenic enzymes and hepatic AMPK activation in SD rats. (**a**) Hepatic protein expression of the key gluconeogenic enzymes G6Pase, (**b**) PEPCK-C, (**c**) and PC in saline and metformin-treated rats. (**d**) Ser133 activating phosphorylation of key transcriptional regulator of gluconeogenesis, CREB, in livers of metformin and saline treated rats. (**e**) Liver AMPK activation as determined by phosphorylation of AMPK relative to total AMPK protein. (**f**) Liver ACC activation as determined by phosphorylation downstream of AMPK action. Data are mean ± SEM, (n=6 per group). For statistical analysis, *P* values were calculated by unpaired, two-sided Student's *t*-test and NS = Not significant.

Supplementary Figure 5

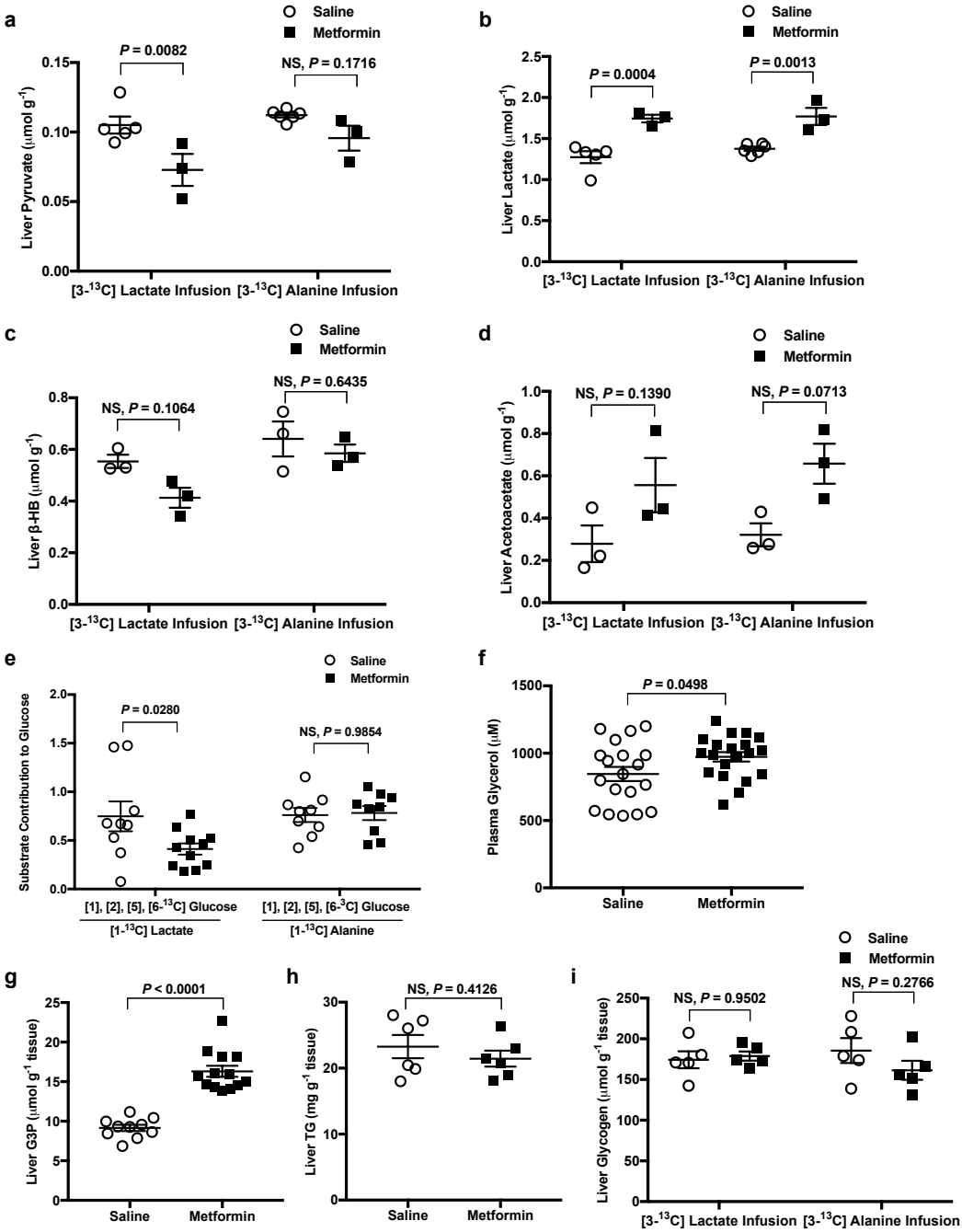

Supplementary Figure 5 Effect of acute IV 50 mg kg^{-1} metformin treatment on liver metabolites in a ZDF rat model of type 2 diabetes. (**a**) Hepatic pyruvate, (**b**) lactate, (**c**) β-hydroxybutyrate and (**d**) acetoacetate concentrations in ZDF rats 2 h post-metformin or saline treatment during both the [3-^{13}C] lactate and [3-^{13}C] alanine tracer infusions. (**e**) Contribution of lactate to hepatic gluconeogenesis as demonstrated by labeling of glucose in positions 1, 2, 5 and 6 by [3-^{13}C]lactate, and alanine contributions observed by labeling of glucose by [3-^{13}C]alanine. (**f**) Plasma glycerol and (**g**) liver G-3-P concentration, (**h**) liver triglyceride levels and (**i**) liver glycogen concentration 2 h post-metformin or saline. Data are mean ± SEM. (For (**a, b**): [3-^{13}C]lactate, saline *n* = 5, metformin *n* = 3, [3-^{13}C]alanine saline *n* = 6, metformin *n* = 3; for (**c, d**): [3-^{13}C]lactate saline *n* = 3, metformin *n* = 3, [3-^{13}C]alanine saline *n* = 3, metformin *n* = 3; for (**e**): [3-^{13}C]lactate saline *n* = 9, metformin *n* = 11, [3-^{13}C]alanine saline *n* = 9, metformin *n* = 9; for (**f**): saline *n* = 20, metformin *n* = 20; for (**g**): saline *n* = 10, metformin *n* = 13; for (**h**): saline *n* = 6, metformin *n* = 6; for (**i**): [3-^{13}C]lactate saline *n* = 5, metformin *n* = 5, [3-^{13}C]alanine saline *n* = 5, metformin *n* = 5; biological replicates). For statistical analysis, *P* values were calculated by two-way *ANOVA* (**a-e, i**) and unpaired, two-sided Student's *t*-test (**f-h**), and NS = Not significant

Supplementary Figure 6

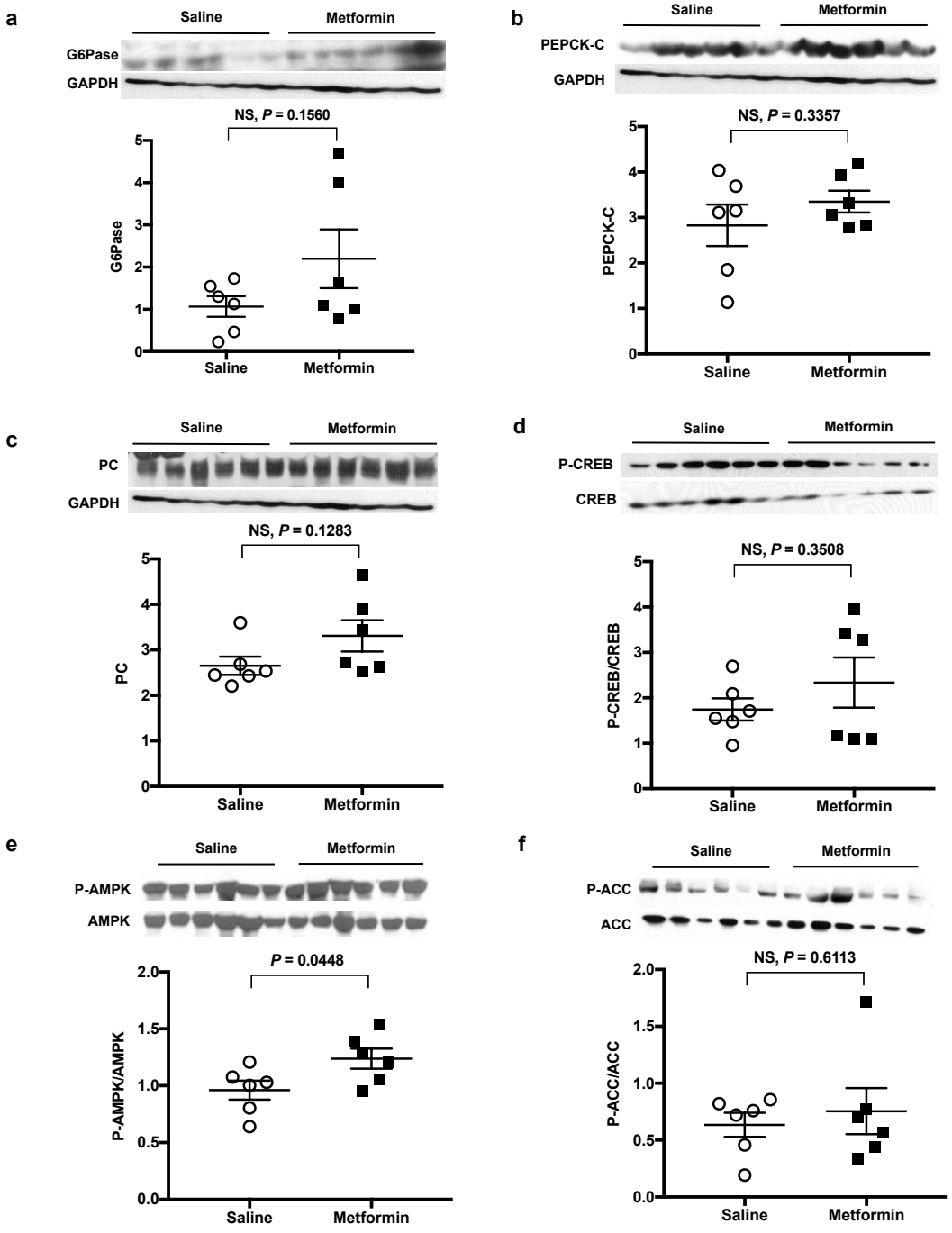

Supplementary Figure 6 Effect of acute IV 50 mg kg^{-1} metformin treatment on the protein expression of liver gluconeogenic enzymes and hepatic AMPK activation in ZDF rats. (**a**) Hepatic protein expression of key gluconeogenic enzymes G6Pase, (**b**) PEPCK-C, (**c**) and PC 2 h post-metformin or saline treatment. (**d**) Activation of CREB as determined by the ratio of phosphorylated CREB to total CREB protein in hepatic tissue. (**e**) Liver AMPK activation as determined by the ratio of phosphorylated AMPK to total AMPK. (**f**) Liver ACC activation as determined by the ratio of phosphorylated ACC to total ACC. Data are mean ± SEM, (n=6 per group). For statistical analysis, *P* values were calculated by unpaired, two-sided Student's *t*-test and NS = Not significant.

Supplementary Figure 7

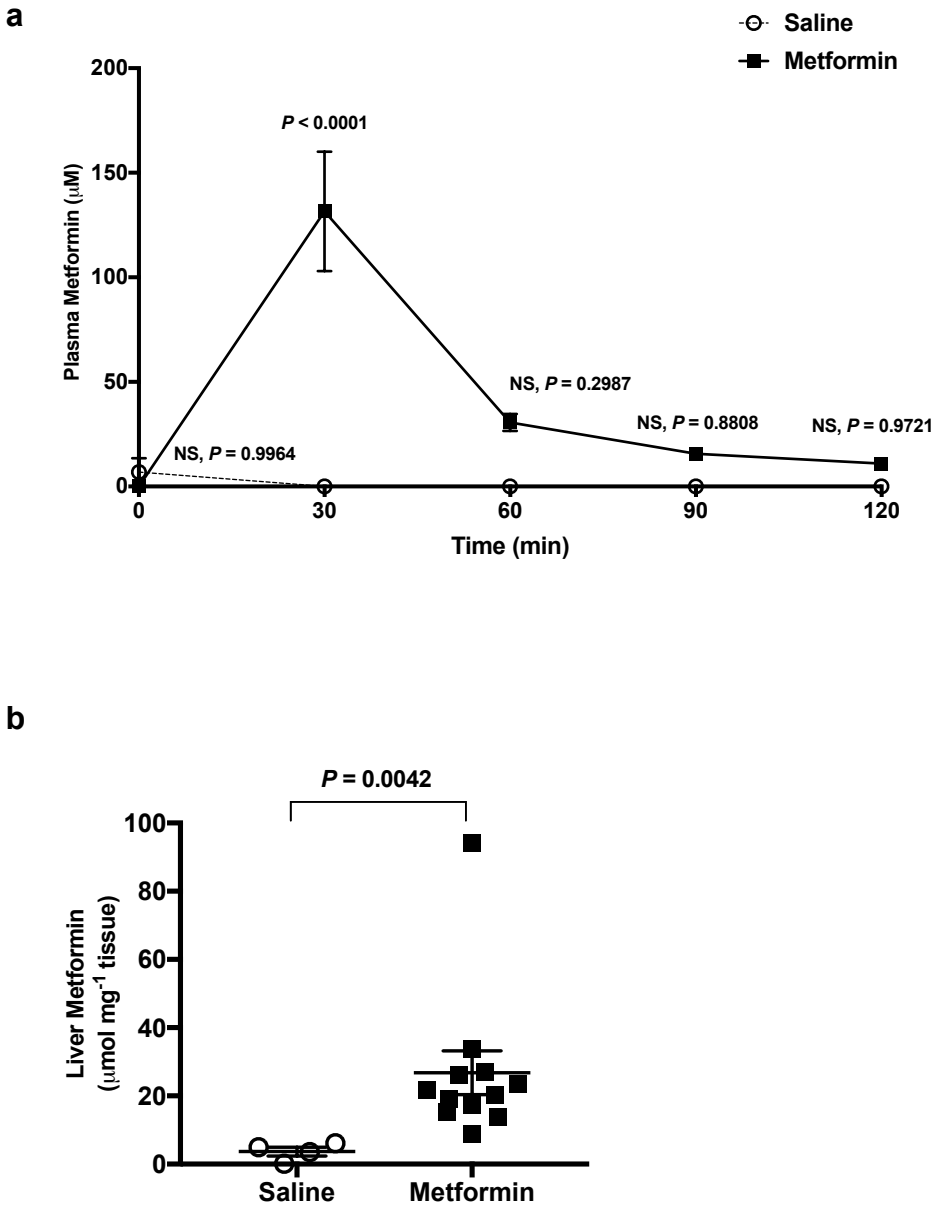

Supplementary Figure 7 Plasma and liver metformin concentrations in a HFD-STZ rat model of type 2 diabetes administered acute portal vein infusions of metformin. (**a**) Rats were placed on a 4-wk HFD and treated with streptozotocin-nicotinamide to ablate the pancreatic β-cells were then treated with 50 mg kg^{-1} metformin by portal vein infusion. Plasma metformin concentrations were measured every 30 minutes over the following 2 hours. (**b**) Liver metformin concentrations were measured 2 hours after acute portal vein treatment with 50 mg kg^{-1} metformin. Data are mean ± SEM. (For (**a**): saline n = 4, metformin n = 6; for (**b**): saline n = 4, metformin n = 12). For statistical analysis, P values were calculated by two-way ANOVA (**a**) and unpaired, two-sided Student's t-test (**b**) and NS = Not significant.

Supplementary Figure 8

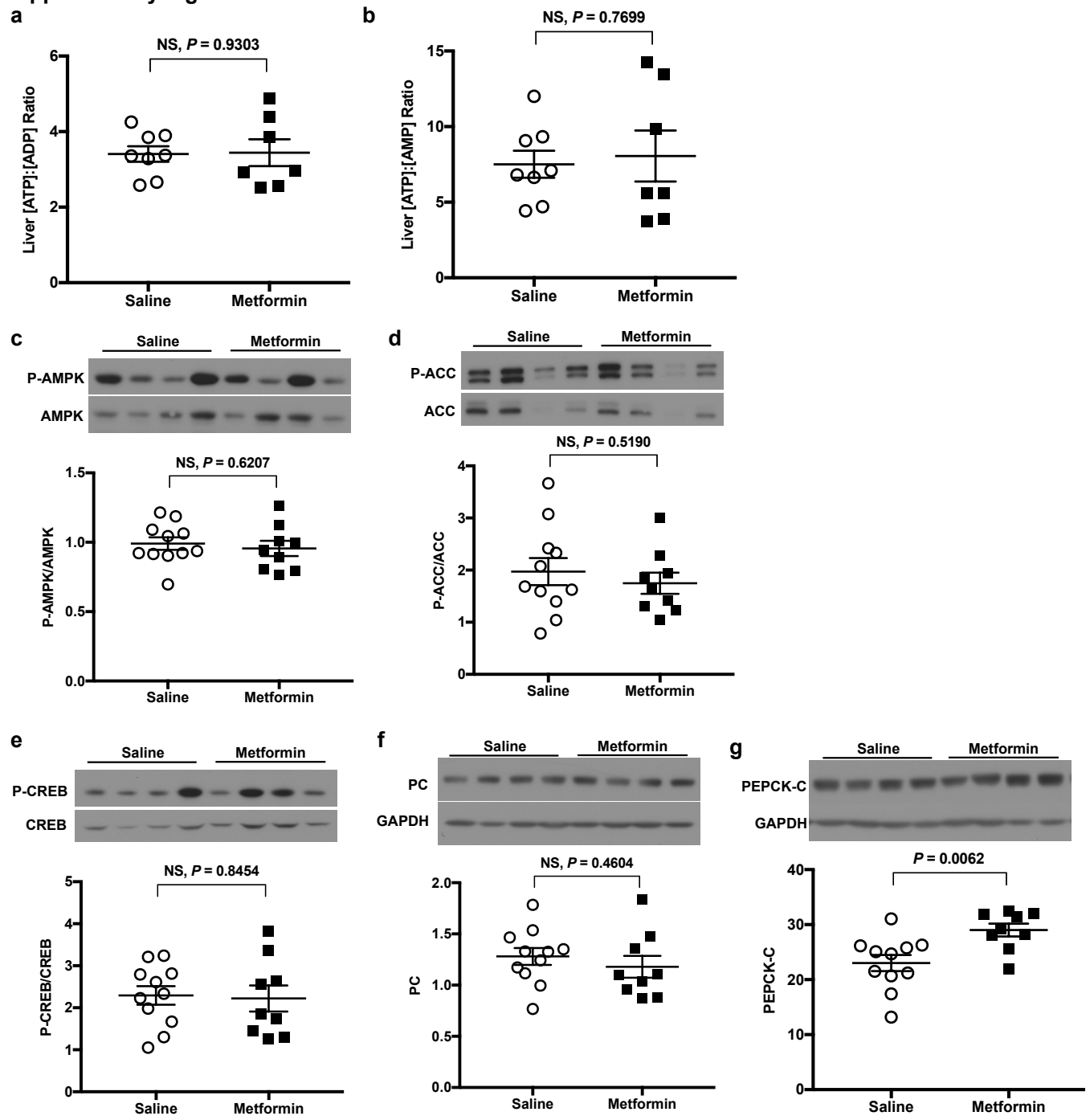

Supplementary Figure 8 Effect of acute portal vein metformin infusion on hepatic energy charge, hepatic gluconeogenic enzyme protein expression and AMPK activation in a HFD-STZ rat model of type 2 diabetes. (**a**) Hepatic [ATP]:[ADP] and (**b**) [ATP]:[AMP] ratios, representative of energy charge, in rats 2 h post- intraportal metformin or saline. (**c**) Hepatic AMPK activation as determined by the ratio of phosphorylated AMPK to total AMPK protein. (**d**) Liver ACC activation determined by the ratio of phosphorylated ACC to total ACC protein. (**e**) Activation of CREB as determined by the ratio of phosphorylated CREB to total CREB protein. (**f**) Liver protein expression of PC and (**g**) PEPCK-C. Data are mean ± SEM. (For (**a, b**): saline n = 8, metformin n = 7; for (**c-g**): saline n = 10, metformin n = 10, blots shown are representative and quantitation was done for full data set). For statistical analysis, P values were calculated by unpaired, two-sided Student's t-test and NS = Not significant.

Supplementary Figure 9

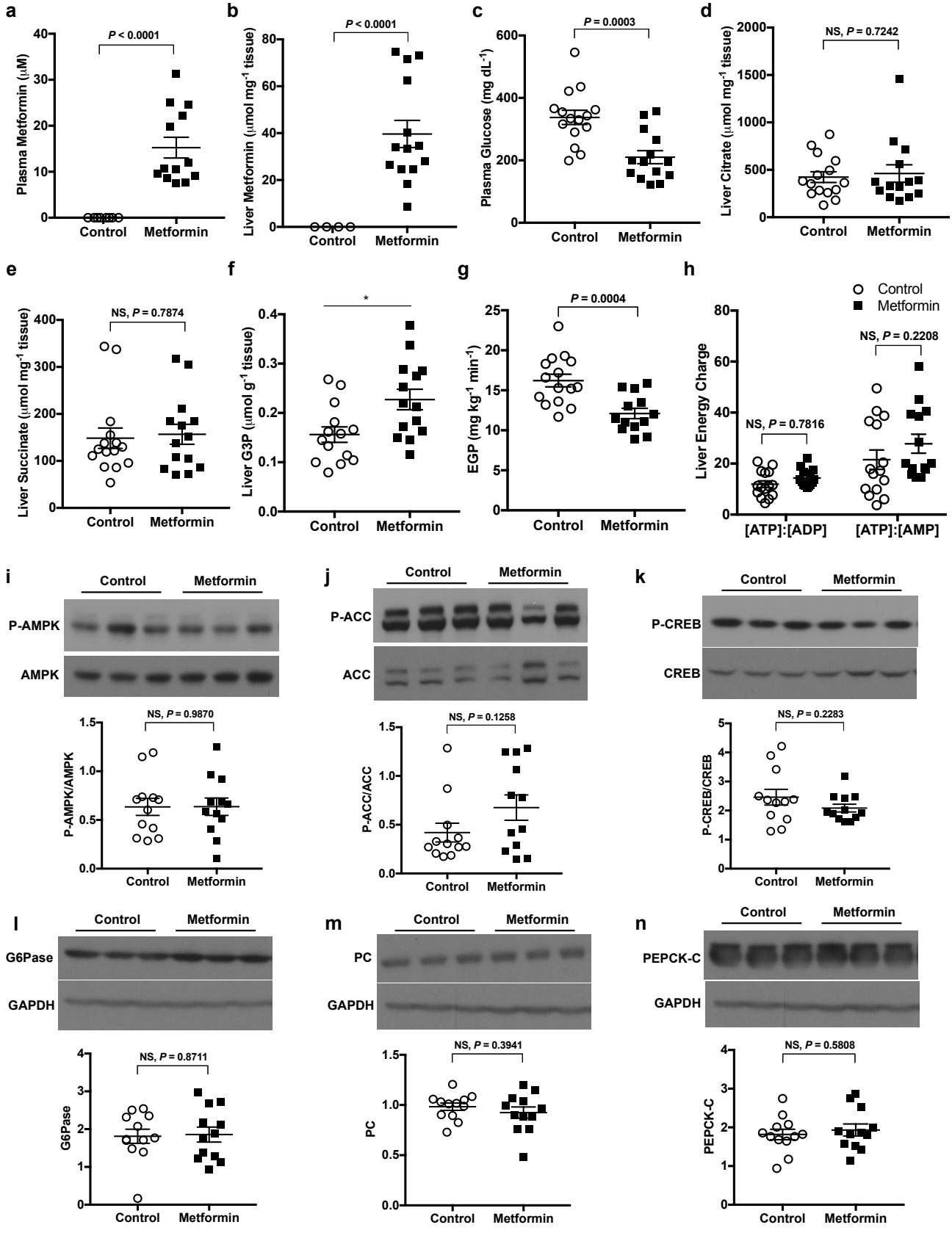

Supplementary Figure 9 Chronic oral metformin treatment in the drinking water (0.5 mg ml^{-1} for 7 days, 1.8 mg ml^{-1} for 7 days and finally 2.7 mg ml^{-1} for 14 days) decreases fasting plasma glucose and endogenous glucose production (EGP) in a ZDF rat model of type 2 diabetes without affecting hepatic energy charge, altering gluconeogenic enzyme protein expression or AMPK activation. (**a**) Plasma metformin and (**b**) hepatic metformin concentrations measured in ZDF rats treated with chronic oral metformin. (**c**) Fasting plasma glucose in ZDF rats administered chronic oral metformin treatment compared to untreated control animals. (**d**) Liver citrate, (**e**) succinate, and (**f**) G-3-P concentrations. (**g**) EGP rates from ZDF rats treated chronically with oral metformin compared with untreated controls. (**h**) Hepatic energy charge as determined by the [ATP]:[ADP] and [ATP]:[AMP] ratios. (i) AMPK phosphorylation, (**j**) ACC phosphorylation, and (**k**) CREB phosphorylation relative to total protein expression in the liver of metformin-treated or untreated ZDF rats. (**l**) Liver protein expression of G6Pase, (**m**) PC and (**n**) PEPCK-C. Data are mean ± SEM, (For (**a**): control n = 8, metformin n = 13; for (**b**): control n = 4, metformin n = 14; for (**c-e, f**): control n = 15, metformin n = 14; for (**f**), control n = 14, metformin n = 14; for (**g**): control n = 15, metformin n = 13; for (**i-n**): control n = 12, metformin n = 12). For statistical analysis, P values were calculated by unpaired, two-sided Student's t-test (**a-g**, **i-n**) and two-way ANOVA (**h**) and NS = Not significant.

Supplementary Figure 10

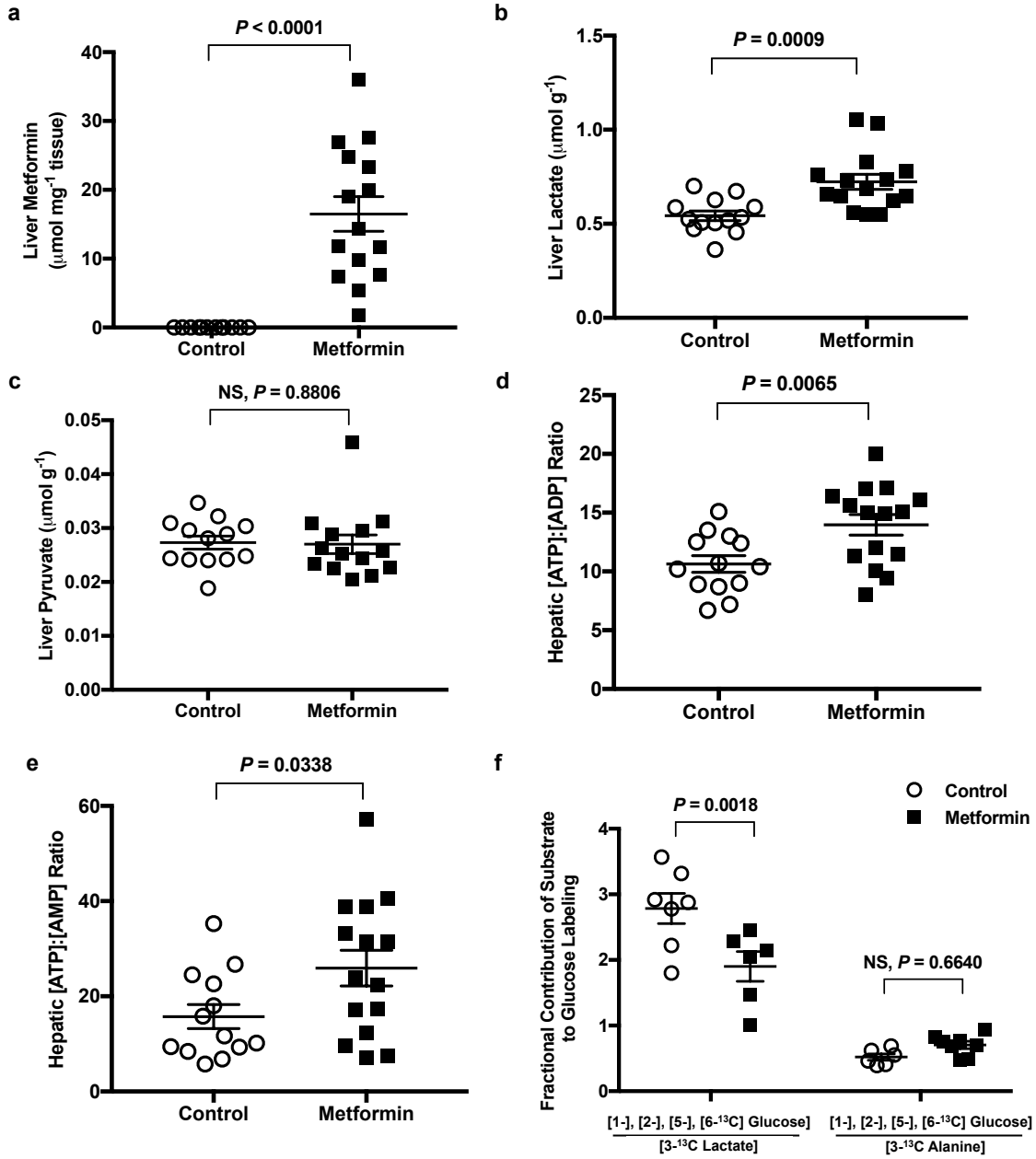

Supplementary Figure 10 Chronic oral metformin treatment in a HFD-STZ rat model of type 2 diabetes specifically decreases contributions of lactate to hepatic gluconeogenesis while increasing the hepatic cytosolic redox state but without decreasing hepatic energy charge at clinically relevant plasma metformin concentrations. (a) A treatment regimen of 200 mg kg^{-1} metformin orally per day for 14 days gave rise to liver metformin concentrations of ~15 μmol mg^{-1}. (b) Liver lactate concentrations were significantly increased by metformin treatment, though (c) there was no impact on hepatic pyruvate concentration. In this rat model, hepatic energy charge was not decreased but in fact modestly but significantly elevated by metformin treatment as demonstrated by (d) an increased [ATP]:[ADP] ratio and (e) increased [ATP]:[AMP] ratio. (f) Lactate contribution to hepatic gluconeogenesis was decreased by metformin compared with saline, shown by diminished labeling of glucose in the 1, 2, 5 and 6 positions by [3-^{13}C]lactate; metformin did not impact the contribution of alanine to gluconeogenesis, evidenced by an absence of change in ^{13}C glucose labeling by [3-^{13}C]alanine. Data are mean ± SEM, (panel (a), control: n=12, metformin: n=15; panel (b, d, e), control: n=13, metformin: n=15; panel (c), control: n=13, metformin: n=14; panel (f), [3-^{13}C] lactate infusion, control: n=7, metformin: n=6, [3-^{13}C] alanine infusion, control: n=6, metformin: n=8. For statistical analysis, *P* values were calculated by unpaired, two-sided *t*-test (**a-e**) and two-way *ANOVA* (**f**) and NS = Not significant.

Supplementary Figure 11

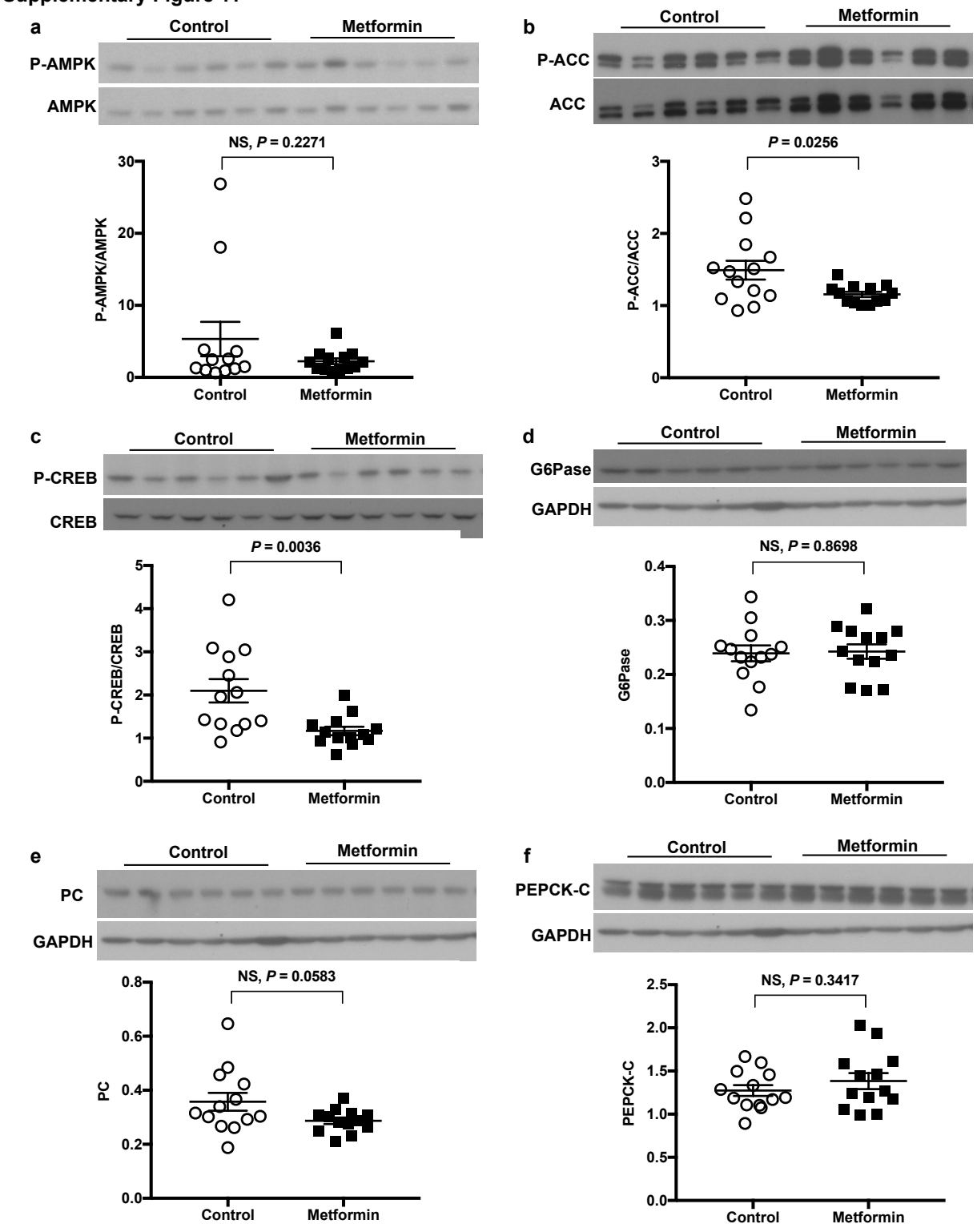

Supplementary Figure 11 Chronic oral metformin treatment of HFD-STZ type 2 diabetes rats does not impact AMPK pathway or gluconeogenic enzyme expression in liver. (**a**) Phosphorylation of AMPK (**b**) AMPK target ACC and (**c**) phosphorylation of CREB in livers of chronically treated HFD-STZ rats. Hepatic protein expression levels of (**d**) G6Pase, (**e**) PC and (**f**) PEPCK-C. Data are mean ± SEM. (For (**a**): control *n* = 12, metformin *n* = 13; for (**b-f**): control *n* = 13, metformin *n* =13). For statistical analysis, *P* values were calculated by unpaired, two-sided Student's *t*-test and NS = Not significant.